Efficient modelling of mid to high frequency underwater acoustic propagation

Alec J Duncan (1), Iain M Parnum (1) and Peter J Henley (2)

(1) Centre for Marine Science and Technology, Curtin University, Western Australia
(2) Maritime Division, Defence Science and Technology Organisation, Western Australia

ABSTRACT

Accurate prediction of the acoustic interference field at mid to high frequencies is computationally intensive, even for ray theory based models, and is of little practical use because the fine detail of the interference pattern is sensitive to the exact values of environmental parameters, such as bathymetry and sound speed, that are inherently uncertain. This paper considers an alternative approach in which a much faster incoherent beam model is used to compute the mean acoustic field, and the interference is treated as a statistical process based on a Rayleigh amplitude distribution. Excellent agreement was found between interference field statistics obtained using this hybrid approach, and those resulting from a full coherent transmission loss calculation whenever the horizontal separation between source and receiver was sufficiently large that there were many contributing ray paths.

INTRODUCTION

Ray theory based acoustic propagation models have been in use for many years and are described in most standard text-books on underwater acoustics. These models have utility at frequencies that are sufficiently high that diffraction and other wave effects can be ignored, and in most practical cases are more computationally efficient at these high frequencies than techniques that retain the full wave propagation physics. For applications such as command decision support tools requiring near real-time acoustic propagation calculations, computational efficiency is paramount and even standard ray theory may be too slow. This paper therefore investigates the feasibility of combining a simplified ray tracing approach with a statistical model of the signal fluctuations as a way of reducing execution time.

The reader is referred to Chapter 3 of Jensen et. al. (2000) for a particularly thorough treatment of ray theory. In summary, the basic principle is to trace the path of each acoustic ray through the ocean while taking appropriate account of refraction and reflection effects. (A ray is a line that is everywhere perpendicular to acoustic wavefronts.) A plot of the resulting ray paths is referred to as a ray trace and provides a useful intuitive picture of the way in which acoustic energy travels in the ocean. An example ray trace is shown in Figure 1.

Early ray models determined the amplitude of the received signal relative to the transmitted signal by comparing the separation between a pair of adjacent rays as they passed the receiver to their separation at a standard distance from the source. The amplitude ratio could then be simply determined from a consideration of the resulting geometrical spreading.

The main disadvantage of this method is that it leads to unphysical predictions of infinite amplitude where initially adjacent rays cross, which is quite common in practice. Locations where this occurs are called caustics. It also predicts zero amplitude in so-called shadow zones where no rays penetrate, whereas in reality diffraction effects would ensure that there was some acoustic energy in these zones.

Gaussian beam models are a more recent development of ray theory intended to address these shortcomings (Porter, 1987, Jensen et. al 2000), and instead treat each ray as the centre of a beam with a Gaussian intensity profile. The signal at the receiver is obtained by summing the contributions of all beams that pass sufficiently close to the receiver to make a significant contribution to the received signal.

In order to calculate the acoustic interference pattern it is necessary to properly calculate the phase of the signal along each ray path. The contributions from different rays are then summed to obtain the coherent received pressure:

$$p_c = \sum_{k=1}^{N} p_k \tag{1}$$

where p_k is the complex pressure at the receiver due to ray $k \in \{1 \ldots N\}$.

If the detailed interference pattern is not required, then the signal phase can be ignored, and the incoherent sum of the received pressure from each ray can be calculated using:

$$p_i = \sqrt{\sum_{k=1}^{N} |p_k|^2} \tag{2}$$

Keeping track of the phase along the ray requires a smaller computational step, and is therefore more computationally demanding, than determining the signal's amplitude. Consequently, evaluation of p_i is significantly faster than the evaluation of p_c, however p_i does not include the fluctuations in received levels due to interference effects and therefore does not give a good indication of likely minimum and maximum received levels.

Figure 2 illustrates this effect with a plot of the coherent and incoherent transmission losses as a function of range for a shallow-water propagation scenario with parameters listed in

Table 1. (The seabed was modelled as a fluid.) Here the coherent transmission loss is defined as:

$$TL_c = -20\log_{10}\left(\frac{|p_c|}{|p_1|}\right) \qquad (3)$$

and the incoherent transmission loss as:

$$TL_i = -20\log_{10}\left(\frac{p_i}{|p_1|}\right) \qquad (4)$$

where p_1 is the source pressure referred to a distance of 1 m from the source.

Tests carried out by the authors (Parnum and Duncan, 2008) using the Gaussian beam tracing model, BELLHOP (Porter, 2011), indicated that a coherent transmission loss calculation typically took 3.3 times longer than an incoherent transmission loss calculation using the same number of beams. Depending on the accuracy required, there was still further scope for speeding up the incoherent calculation by reducing the number of beams.

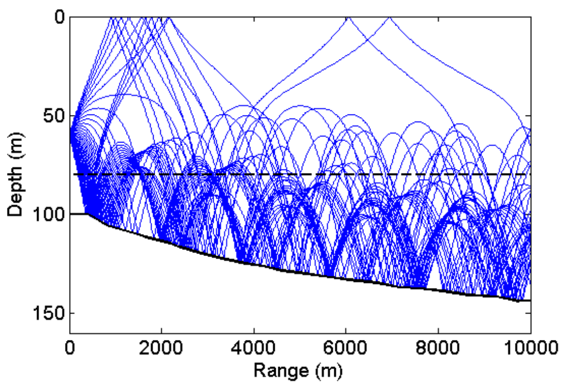

Figure 1. Ray trace plot for the test scenario described in Table 1. The broken horizontal black line is at the receiver depth. The solid black line is the seabed.

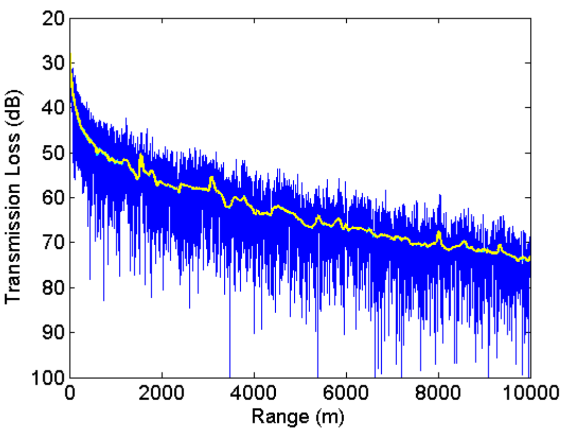

Figure 2. Comparison between coherent (blue) and incoherent (yellow) transmission loss at a frequency of 7 kHz for the shallow water propagation scenario described in Table 1 and Figure 3.

The results in figures 1 and 2 were calculated using BELLHOP. As well as coherent and incoherent transmission loss, BELLHOP can calculate what is referred to as the semi-coherent transmission loss. This is the incoherent transmission loss with the effect of the interference between the direct and surface reflected paths included by an analytic modulation of the beam amplitudes. However for a source many wavelengths deep, as in this case, the incoherent and semicoherent transmission loss curves are indistinguishable.

Table 1. Test scenario parameters

Parameter	**Value**
Acoustic frequency	7 kHz
Source depth	60 m
Receiver depth	80 m
Water depth	100m to 140m (Fig. 1)
Maximum range	10000 m
Water column sound speed	Downward refracting (Fig. 3)
Water column density	1024 kg.m^{-3}
Seabed sound speed	1750 m.s^{-1}
Seabed attenuation	0.8 dB.λ^{-1}
Seabed density	1941 kg.m^{-3}

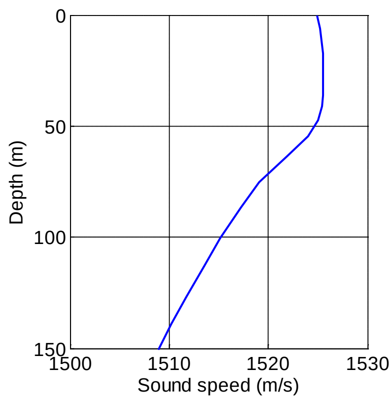

Figure 3. Sound speed profile for the test scenario used in this paper.

As mentioned above, this study explores the concept of treating the signal fluctuations due to destructive and constructive interference as a random process superimposed on the incoherent or semicoherent transmission loss. This allows the probability of a received level being exceeded at a given range to be determined by a relatively fast incoherent transmission loss calculation, followed by a consideration of the appropriate probability distribution. A justification for pursuing this approach is provided by figures 4 and 5, which show expanded views of two sections of Figure 2. There are substantial fluctuations in the incoherent transmission loss due to the ray convergence zones seen in Figure 1, but in most cases the coherent transmission loss tracks these fluctuations.

STATISTICS OF AMPLITUDE AND SIGNAL LEVEL FLUCTUATIONS

The statistics of the acoustic inteference field were considered in detail by Dyer (1970). The fundamental concept is that if sound arrives at a receiver via a sufficient number of different paths with a random phase relationship then the combined signal's in-phase and quadrature components will be Gaussian distributed, its amplitude fluctuations will be

Rayleigh distributed; and the signal level (in decibels) will be log-Rayleigh distributed (Shepherd & Milnarich Jr 1973).

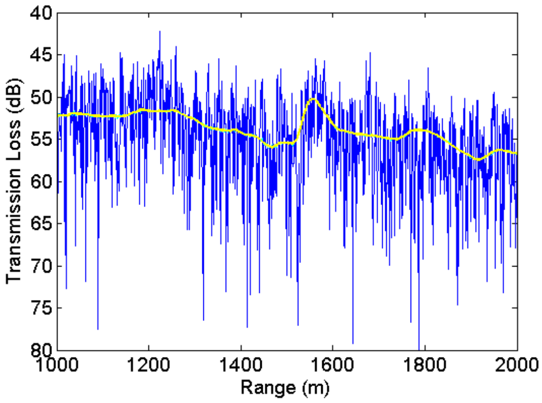

Figure 4. Expanded view of Figure 2 showing only ranges from 1000m to 2000m.

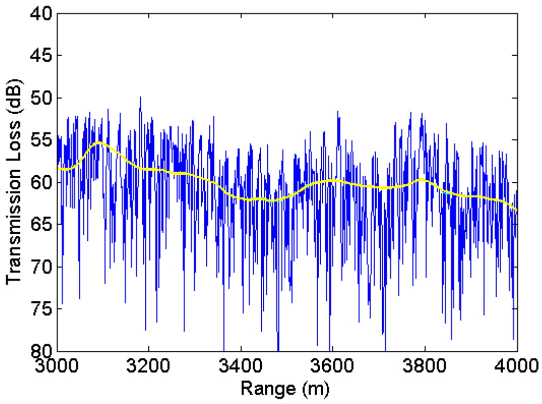

Figure 5. Expanded view of Figure 2 showing only ranges from 3000m to 4000m.

The probability density function (PDF) of a Rayleigh distribution is defined by Equation (5).

$$f(x \mid b) = \frac{x}{b^2} \exp\left(\frac{-x^2}{2b^2}\right) \tag{5}$$

Where the probability density of *x* is computed for the value of the Rayleigh parameter, *b*.

The mean of the Rayleigh distribution is:

$$\mu_R = b\sqrt{\frac{\pi}{2}} \tag{6}$$

When converting an amplitude measure, x, to a decibel level *y*, we apply the formula:

$$y = K \log_{10} x = \frac{2}{\alpha} \ln x \tag{7}$$

Where $K = 20$ and

$$\alpha = \frac{2\ln 10}{K} = 0.2303 \tag{8}$$

The PDF for y can be shown to be (Shepherd and Milnarich, 1973):

$$f(y \mid b) = \frac{\alpha}{2b^2} \exp\left[y\alpha - \frac{\exp(y\alpha)}{2b^2}\right] \tag{9}$$

and the corresponding cumulative distribution function is:

$$F(y \mid b) = 1 - \exp\left[-\frac{\exp(y\alpha)}{2b^2}\right] \tag{10}$$

An interesting property of the log-Rayleigh distribution is that, unlike the Rayleigh distribution, the variance is constant and is:

$$\mathrm{var}(y, b) = \frac{1.6449341}{\alpha^2} \tag{11}$$

For the case of $K = 20$ the variance is 31.0 dB^2, giving a standard deviation of 5.6 dB.

If the amplitude of the coherent pressure is Rayleigh distributed with a mean equal to the incoherent pressure then dividing the amplitude of the coherent pressure by the incoherent pressurewill yield a Rayleigh distributed random variable with a mean of 1, which from Equation (6) gives $b = \sqrt{2/\pi}$.

The probability that a received level, L_{RC}, exceeds the received level predicted using the incoherent transmission loss, L_{RI}, by more than T dB would therefore be given by:

$$\Pr(L_{RC} - L_{RI} > T) = 1 - F(T \mid b) \tag{12}$$

with α = 0.2303 and b = 0.7979, and where $F(T \mid b)$ is given by Equation (10).

Equation (12) is plotted in Figure 6. Note that this result differs somewhat from that given in Duncan and Parsons (2011), which was based on a Rayleigh parameter of $b = \sqrt{1/2} = 0.7071$.

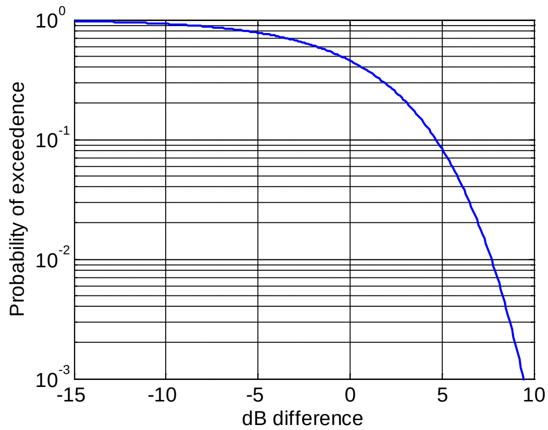

Figure 6. Probability that the received level exceeds the level calculated using the incoherent transmission loss by the specified number of dB. Assumes that the amplitude of the coherent pressure is Rayleigh distributed with a mean equal to the incoherent pressure.

TESTS WITH MODELLED DATA

The downslope propagation scenario described above was used to test this approach. This scenario was chosen because the strong ray convergence features visible in Figure 1, and the resulting fluctuations in the incoherent transmission loss that are clearly seen in figures 2, 4, and 5, make this a fairly severe test case.

BELLHOP was used to calculate the incoherent and coherent received pressure for unit source amplitude as a function of range, at 1m intervals from 10m to 10km. The amplitude of the coherent pressure was normalised by dividing by the incoherent pressure and then converting to decibels to give normalised coherent received levels. The resulting levels were extracted for 100m range intervals and then histogrammed, with the histograms scaled to unit area for comparison with the expected PDF. This PDF is given by Equation (9) with α = 0.2303 and b = 0.7979, and has no fitted parameters.

Results are plotted in Figure 7 for a number of different ranges and show good agreement between the histograms and the expected Log-Rayleigh distribution, except in the first 100m. At this short range the received level is dominated by the direct path signal, whereas the application of the Log-Rayleigh distribution to this problem assumes many ray paths of similar amplitude, so this result is expected. The 1510 m to 1610 m range interval was chosen to demonstrate that the Log-Rayleigh distribution is a good approximation even in one of the ray convergence zones.

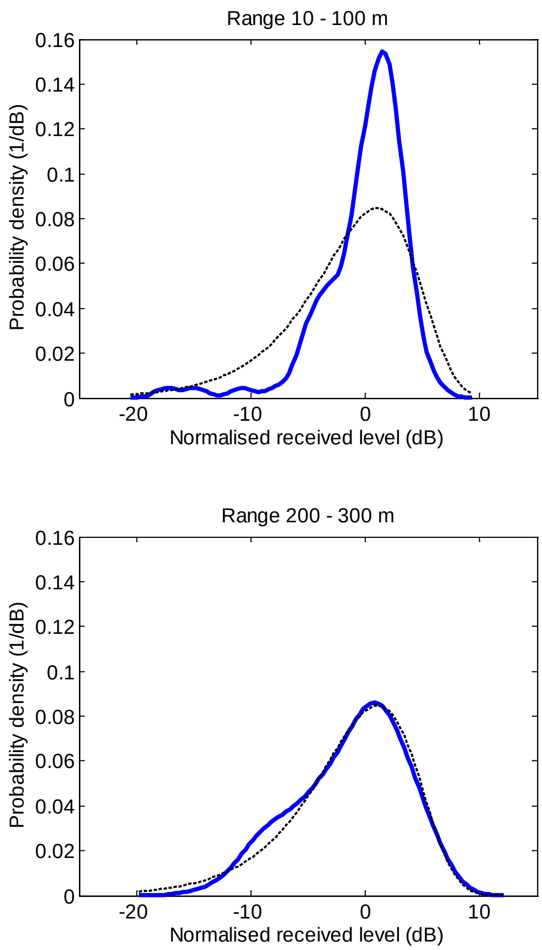

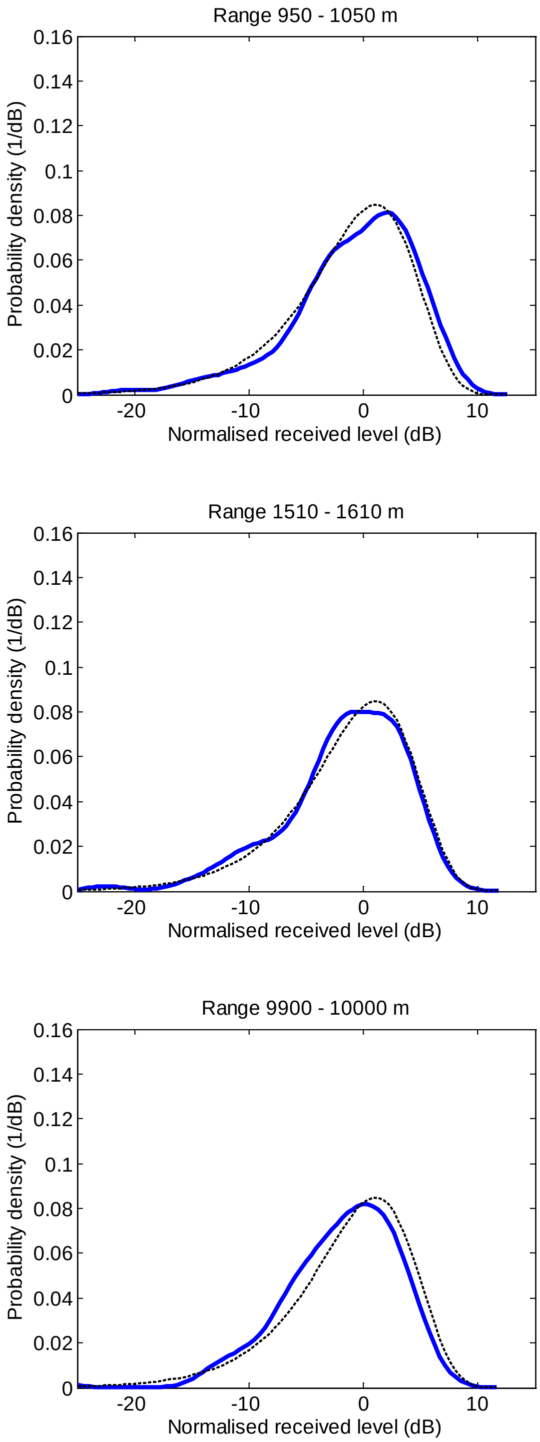

Figure 7. Histograms of normalised coherent received level (solid blue line) for the specified 100 m range bins compared to the expected Log-Rayleigh distribution (dotted black line).

Following Trevorrow (2004), we use the scintillation index, *SI*, as an indicator of whether the normalised coherent pressure is Rayleigh distributed. The scintillation index is defined as:

$$SI = \frac{\mathrm{var}(I)}{\mathrm{mean}(I)^2} \tag{13}$$

where I is the signal intensity. I is proportional to the square of the amplitude of the coherent pressure, p_c, so this is equivalent to:

$$SI = \frac{\mathrm{var}\left(\left|p_c\right|^2\right)}{\mathrm{mean}\left(\left|p_c\right|^2\right)^2} \qquad (14)$$

and is equal to 1 if $\left|p_c\right|$ is Rayleigh distributed.

SI was estimated using a 1000m sliding range window and is plotted as a function of range in Figure 8. It is seen to be close to 1 at all ranges with a maximum deviation of -0.33 at the minimum modelled range of 10 m.

Another useful test is provided by Equation (11), which shows that the received level calculated using the coherent transmission loss should have a variance of 31.0 dB^2, corresponding to a standard deviation of 5.6 dB.. The standard deviation of the coherent field was calculated using a 1000 m running window and is plotted in Figure 9. Again the results conform well to the expected value for a Log-Rayleigh distributed random variable, and again the largest discrepancy occurs at minimum range.

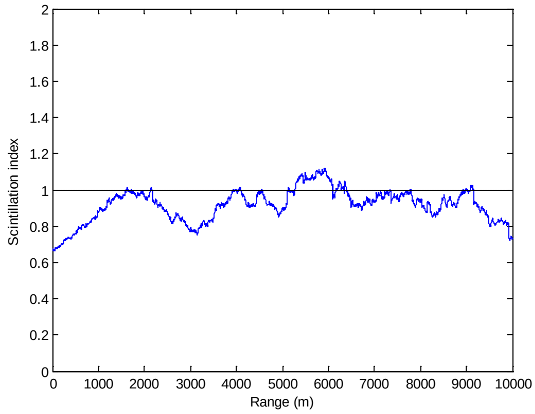

Figure 8. Scintillation Index versus range. Black dashed line represents expected value for a Rayleigh distribution.

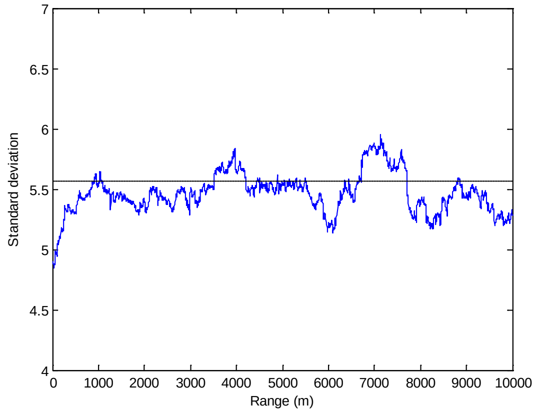

Figure 9. Coherent TL standard deviation versus range, black dashed line represents expected value for a log-Rayleigh distribution.

CONCLUSIONS

The results presented here support the concept of using the incoherent transmission loss along with a Log-Rayleigh distribution as an efficient method of carrying out high frequency received level calculations in situations where the received signal has contributions from many ray paths of similar amplitude.

Similar results have been obtained for a constant depth, isovelocity scenario with a shallow (4 m deep) source. In that case better results were obtained using the semicoherent transmission loss in place of the incoherent transmission loss used here, as the shallow source resulted in predictable interference between the direct and surface reflected paths.

Further work is required to explore the bounds of applicability of the method and particularly to answer such questions as:

- What is the minimum number of ray paths required before a Log-Rayleigh distribution becomes an adequate approximation?
- Can another probability distribution (e.g. a Rician distribution) be used to extend the method to shorter range?

ACKNOWLEDGEMENTS

This work was supported by the Maritime Division of the Defence Science and Technology Organisation.

REFERENCES

Duncan, AJ & Parsons, MJG, 2011, 'How wrong can you be? Can a simple spreading formula be used to predict worst-case underwater sound levels?', *Proc. Acoustics 2011*, 2-4 November 2011, Gold Coast, Australia.

Dyer, I., 1970, 'Statistics of sound propagation in the ocean', *Journal of the Acoustical Society of America*, vol. 48, pp. 337-345.

Jensen, FB, Kuperman, WA, Porter, MB, Schmidt, H, 2000, *Computational Ocean Acoustics*, 2nd Ed., Springer, ISBN 978-1-4419-8677-1.

Parnum , IM and Duncan AJ, 2008, *Sonar Detection Tool-Progress Report*, Centre for Marine Science and Technology, Curtin University, Report 2008-20.

Porter, MB & Bucker, HP 1987, 'Gaussian beam tracing for computing ocean acoustic fields', *Journal of the Acoustical Society of America*, vol. 82, no. 4, pp. 1349-59.

Porter, MB, 2011, *Ocean Acoustics Toolbox*. http://oalib.hlsresearch.com/Modes/AcousticsToolbox/

Shepherd, WL & Milnarich Jr, P 1973, 'Basic Relations Between a Rayleigh-Distributed Randomly Varying Voltage and a Decibel Record of the Voltage', *Proc. IEEE*, vol. 61, no. 12, pp. 1765-6.

Trevorrow, MV, 2004, "Statistics of Fluctuations in High-Frequency Low-Grazing-Angle Backscatter From a Rocky Sea Bed", *IEEE Journal of Oceanic Engineering*, vol. 29, no. 2, pp.236-245.